O3MSAF – SATELLITE APPLICATION FACILITY ON OZONE AND ATMOSPHERIC CHEMISTRY MONITORING

VISITING SCIENTIST 2007

FINAL REPORT

VERIFICATION OF GOME-2 OZONE, NO_2 AND BrO TOTAL COLUMN RETRIEVAL ALGORITHMS

reference / *référence*	
issue / *édition*	1
revision / *révision*	0
date of issue / *date d'édition*	15 Dec 2008

prepared by / *préparé par*	M. Van Roozendael
contributeurs / *contributors*	F. Hendrick, C. Fayt, C. Hermans, N. Theys, D. Loyola, P. Valks, J.-C. Lambert, G. Pinardi, J. van Gent

reference / *référence*	IASB-GOME2-O3MSAF-VS2007
issue / *édition*	1
revision / *révision*	0
status / *état*	Final
date of issue / *date d'édition*	15 Dec 2008
document type / *type de document*	Final report

CONTENTS

ACRONYMS AND ABBREVIATIONS 3

A. INTRODUCTION 4

A.1. SCOPE OF THIS DOCUMENT 4
A.2. PRELIMINARY NOTES 4
A.3. PLAN OF THIS DOCUMENT 4

B. O_3 COLUMN VERIFICATION 5

B.1. VERIFICATION AND VALIDATION TASKS 5
B.2. O_3 ABSORPTION CROSS-SECTIONS FOR USE WITH GOME-2 5
B.3. TOTAL OZONE VERIFICATION IN EQUATORIAL REGION 7
B.4. EAST – WEST BIAS PROBLEM 8

C. NO_2 COLUMN VERIFICATION 10

C.1. NO_2 SLANT COLUMN VERIFICATION 10
C.2. PRELIMINARY VALIDATION OF NO_2 VERTICAL COLUMNS 11

D. BRO COLUMN VERIFICATION 14

D.1. SETTINGS FOR BRO COLUMN RETRIEVAL FROM GOME-2 14
D.1.1. Experience from ERS-2 GOME and SCIAMACHY *14*
D.1.2. Choice of BrO slant column settings for GOME-2 ..... *14*
D.2. VERIFICATION OF BRO SLANT COLUMNS AND SENSITIVITY TESTS 16
D.3. COMPARISON AGAINST SATELLITE DATA 19
D.4. COMPARISON AGAINST GROUND-BASED MEASUREMENTS 23
D.5. SENSITIVITY OF GOME-2 BRO RETRIEVALS TO DOAS SETTINGS CHANGES 24

E. CONCLUSIONS 27

F. REFERENCES 28

F.1. PEER-REVIEWED ARTICLES AND CONFERENCE PROCEEDINGS 28
F.2. TECHNICAL NOTES 29

ACRONYMS AND ABBREVIATIONS

AMF	Air Mass Factor, or optical enhancement factor
BIRA-IASB	Belgian Institute for Space Aeronomy
BrO	bromine monoxide
DLR	German Aerospace Centre
DOAS	Differential Optical Absorption Spectroscopy
ENVISAT	Environmental Satellite
ERS-2	European Remote Sensing Satellite -2
ESA	European Space Agency
EUMETSAT	European Organisation for the Exploitation of Meteorological Satellites
FMI	Finnish Meteorological Institute – Arctic Research Centre
GB-DOAS	Ground-based DOAS instruments
GDOAS	GOME DOAS algorithm developed at BIRA-IASB
GDP	GOME Data Processor
GOME	Global Ozone Monitoring Experiment
IMF	Remote Sensing Technology Institute
NDACC	Network for the Detection of Atmospheric Composition Change
NO_2	Nitrogen dioxyde
O3M-SAF	Ozone and Atmospheric Chemistry Monitoring Satellite Application Facility
OMI	Ozone Monitoring Instrument
QBO	Quasi-biennial oscialltion
ROCINN	Retrieval of Cloud Information using Neural Networks
SCD	Slant Column Density
SCIAMACHY	Scanning Imaging Absorption spectroMeter for Atmospheric CHartography
SCIATRAN	Radiative transfer model developed in Bremen for the SCIAMACHY mission
SZA	Solar Zenith Angle
TEMIS	Tropospheric Emission Monitoring Internet Service
UPAS	Universal Processor for UV/VIS Atmospheric Spectrometers
VCD	Vertical Column Density
WMO	World Meteorological Organization

A. INTRODUCTION

A.1. Scope of this document

This document reports on results achieved as part of the O3-SAF visiting scientist project entitled "Verification of GOME-2 Ozone, NO_2 and BrO Total Column Retrieval Algorithms". It includes verification and validation work performed at BIRA-IASB in support of the development of the operational trace gas data products generated at DLR.

A.2. Preliminary notes

We first report on the verification of the operational GOME-2 trace gas column data against correspondent data sets generated using synchronised scientific algorithm available at BIRA-IASB. For these exercises, retrieval settings jointly selected with DLR based on past experience are being used. The consistency of the O3, NO2 and BrO products are explored by performing comparisons with a selection of correlative data sets, including where relevant scientific data sets from ERS-2 GOME and ENVISAT SCIAMACHY. In the case of BrO, of which the validation is not specifically addressed in the O3-SAF validation programme, ground-based column measurements are also used in an attempt to further document the geophysical consistency of the GOME-2 demonstration product. Note that the BrO validation results presented here must be considered as preliminary and therefore subject to possible revisions.

Reported validation studies were carried out at the Belgian Institute for Space Aeronomy (IASB-BIRA, Brussels, Belgium) and at DLR Remote Sensing Technology Institute (DLR-IMF, Oberpfaffenhofen, Germany) in the framework of EUMETSAT Satellite Application Facility on Ozone and Atmospheric Chemistry Monitoring (O3M-SAF)

A.3. Plan of this document

This document is divided in three main parts (sections B, C, D), addressing respectively total ozone, total NO2 and total BrO data products. Concluding remarks are given in section E.

B. O_3 COLUMN VERIFICATION

B.1. Verification and validation tasks

Verification in this work relies on tools and experience developed as part of the BIRA-IASB contribution to the ERS-2 GOME mission. Relevant tasks include the provision of recommendations for retrieval settings optimisation and, according to needs, the delivery of reference data sets properly matched to the GOME-2 spectral characteristics (molecular absorption cross-sections and Ring effect spectra). Scientific retrieval tools available at BIRA-IASB are synchronised with the UPAS operational system at DLR-IMF. Verification runs are performed on test orbits and results are checked for mutual consistency. GOME-2 retrievals are further cross-checked by comparison to other space sensors (GOME, SCIAMACHY) using same retrieval tools and settings. For the sake of validation, additional comparisons are performed with independent ground-truth or space-based data sets. Comprehensive validation tasks, including assessment of various angular, geometrical and geophysical dependencies (SZA, clouds, season, latitude, etc) are beyond the scope of the present VS project.

B.2. O_3 absorption cross-sections for use with GOME-2

Ozone absorption cross-sections are key input data for total ozone retrieval from GOME-2. In this work, several possible reference absorption cross-section data sets have been tested as to their suitability for GOME-2 retrievals. This included:

- GOME-2 flight-model measurements (G2FM3_V2)
- GOME FM98 data set (GFM98, Burrows et al., 1999)
- Bass & Paur (Bass and Paur, 1985; Paur and Bass, 1985)
- Brion (Daumont et al., 1992; Brion et al., 1993, 1998; Malicet et al., 1995)

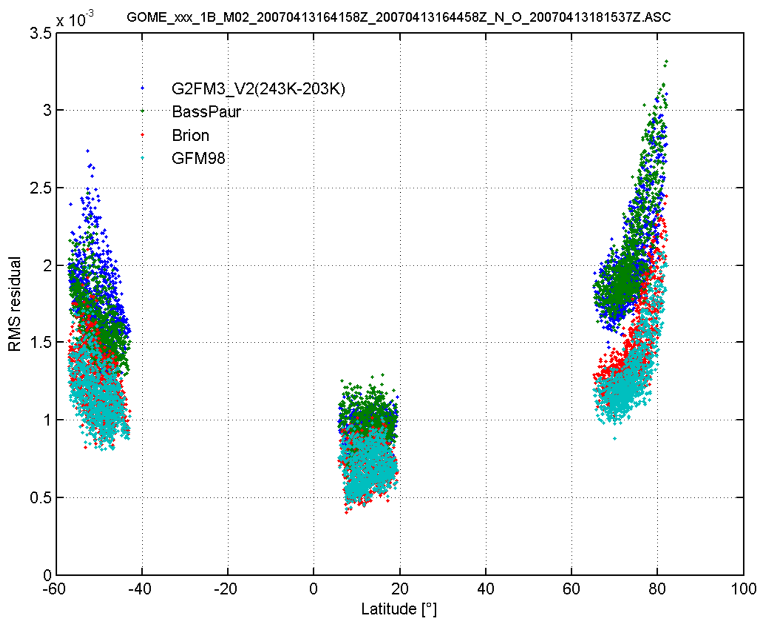

Figure B.1. Residuals of GOME-2 total ozone slant column fits, for different absorption cross-section reference data sets. O_3 slant columns are retrieved in the 325-335 nm interval

Results from test DOAS retrievals performed in the spectral range 325-335 nm are summarised in Figures B.1 to B.4. As can be seen, best residuals are found using the original GOME FM98 data set (adequately smoothed to the resolution of GOME-2). GOME-2 FM (G2FM3_V2) differential cross-sections are approximately 3 % smaller than GFM98 and thus give larger O_3 slant columns (Figure B.2). G2FM3_V2 are in good agreement with Brion data. Note however that the G2FM3_V2 cross-sections at 223°K are inconsistent with those given at other temperatures (see Figure B.3).

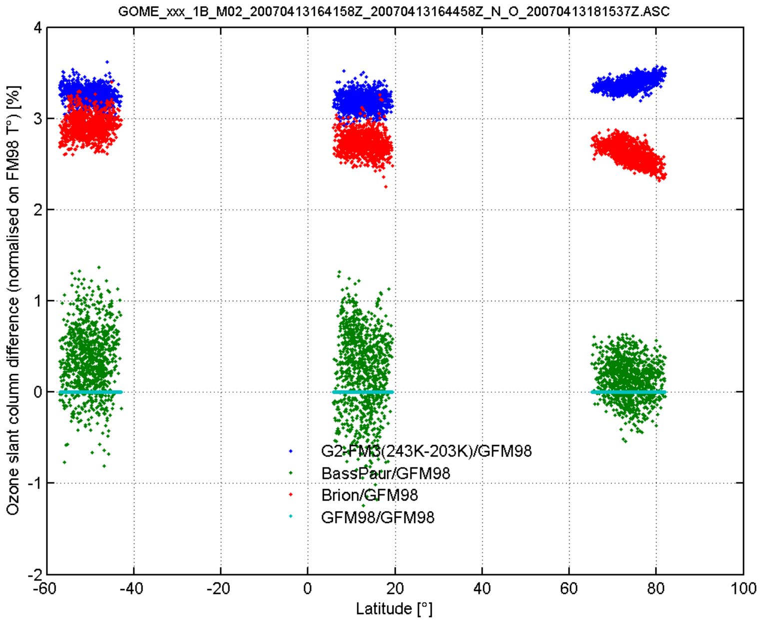

Figure B.2. Relative difference in O_3 slant columns retrieved using different absorption cross-section data sets.

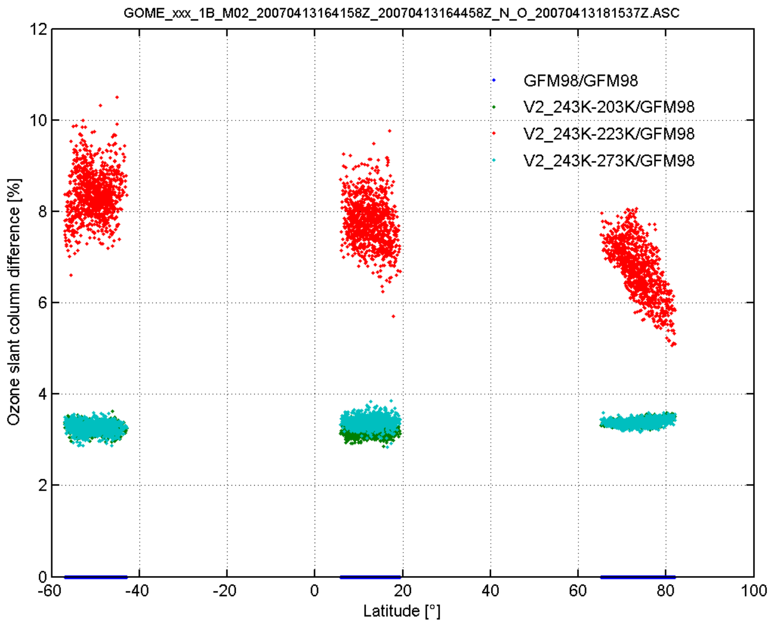

Figure B.3. Relative difference in O_3 slant columns retrieved using different combinations of the G2FM3_V2 absorption cross-sections, in comparison to GOME FM98.

Bass and Paur data are consistent with GOME FM98, but are more noisy and lead to larger instabilities on the slant column retrieval (see noise on Bass & Paur O_3 columns in comparison to other test retrievals). We also checked the accuracy of the wavelength registration of the different cross-sections. This was obtained by allowing the shift of the O_3 cross-section to vary as part of the DOAS fitting procedure, thus optimising its wavelength alignment with respect to our reference Frauhofer lines atlas (Chance & Spurr). Results indicate that the Brion et al. data set has the most accurate wavelength registration. Other reference cross-sections have shifts in the range of a few hundreds of a percent which must be corrected by application of a suitable pre-shift value.

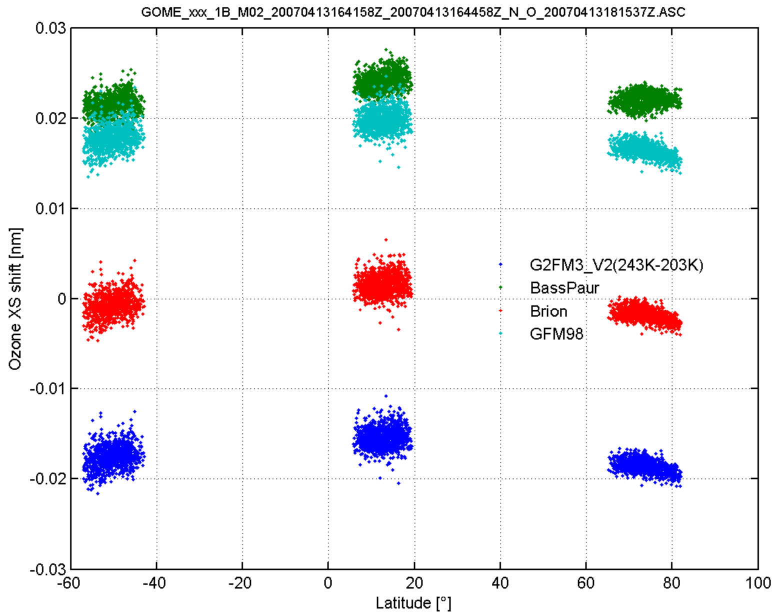

Figure B.4. Shift of the O_3 absorption cross-section, as derived from the DOAS fit procedure.

Given the quality of the O3 fit residuals (Figure B.1) and for the sake of consistency with ERS-2 GOME retrievals by the GDP 4 system, we have recommended the use of GOME FM98 as a baseline for GOME-2 total ozone retrievals.

B.3. Total ozone verification in equatorial region

The BIRA-IASB GDOAS tool has been synchronised with the GDP 4 system. DOAS settings, including O_3 cross-sections but also Ring effect cross-sections accurately smoothed using the GOME-2 slit function, have been implemented in both systems, and verification runs have been performed. In-line with past verification exercises conducted for ERS-2 GOME, very good agreement was found, with differences on slant columns lower than 0.5 %. In the course of the verification, one small problem of discontinuity taking place at the transition between Northern and Southern latitudes was identified (see Figure B.5). This problem was due to a bug in the interpolation of the ozone profile in the GDP 4 system which could be easily fixed. The remaining vertical column differences that can be observed in Figure B.5 are well understood as being dominated by the use of different cloud products (FRESCO for GDOAS, and OCRA/ROCINN for GDP 4). These results illustrate the impact of clouds as limiting factors to the accuracy of total ozone retrieved from UV backscattered radiances.

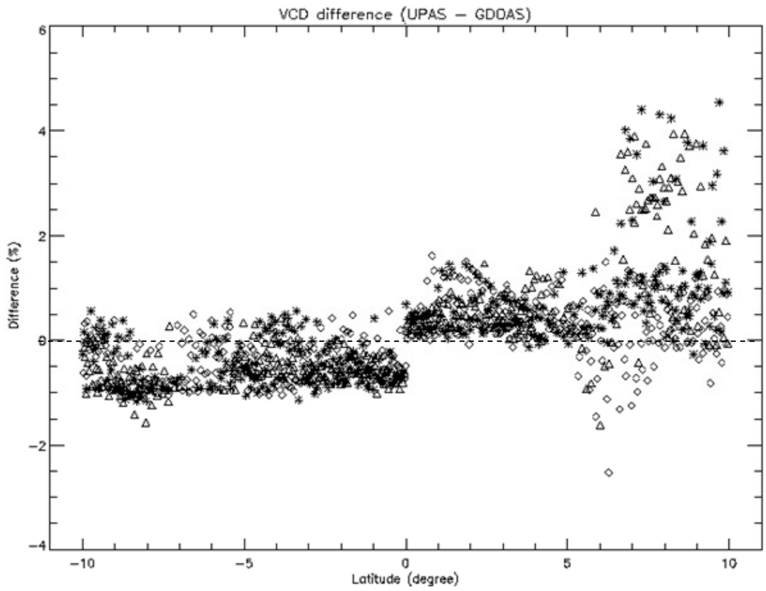

Figure B.5. Comparison of total ozone values retrieved in the equatorial region using the GDOAS and UPAS (GDP 4) systems.

B.4. East – West bias problem

Early evaluation from the UPAS system displayed a tendency for GOME-2 to measure larger O_3 columns on the west-side of the swath than on the east side. This anomaly was similarly identified in verification data sets produced at BIRA-IASB using GDOAS. The problem can be clearly seen in Figure B.6 where tropical O_3 columns are displayed over the Pacific Ocean. DOAS fit residuals are also found to be systematically larger the east side of the orbit.

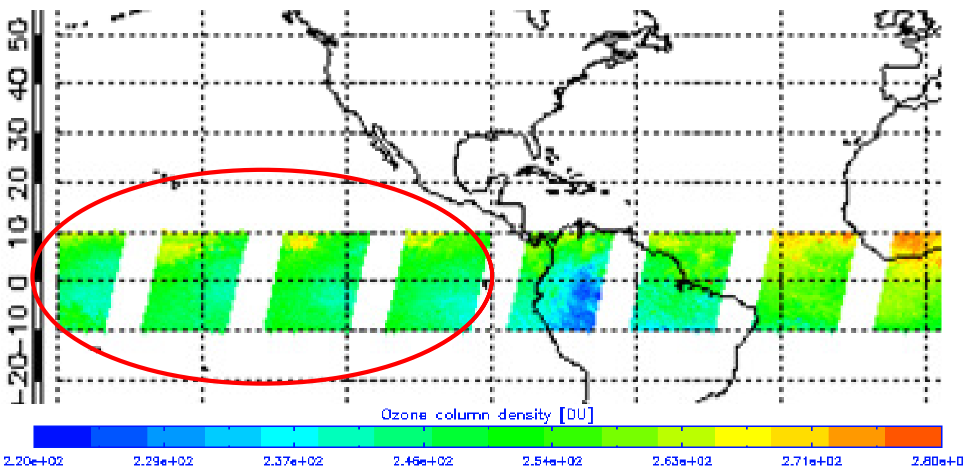

Figure B.6. GDOAS retrievals of total ozone in the Pacific equatorial region. Results show anomalous east-west dependences, with total ozone being systematically smaller on the east side than on the west side of the GOME-2 swath.

Additional test retrievals were performed to better characterise this east-west bias problem. Results are given in Tables B.1 and B.2. For the first tests (Table B.1), differences in ozone columns between east and west pixels and differences in RMS fitting residuals were calculated for different wavelength intervals. Results show that the east-west bias is similar whatever the selected fitting range. Differences in RMS residuals are also similar, except for the interval at shortest wavelengths. But this is not significant since residuals at such short wavelengths are largely dominated by increased noise and larger systematic misfit effects playing similarly on east and west pixels.

Table B.1. Fitting window dependence (data all June 2007)

Window	O_3 VCD % diff	Residual % diff
315-325	-2.17	1.50
325-335	-2.19	11.6
330-340	-1.99	12.8

In a second exercise (Table B.2) the cloud dependency of the retrievals was investigated. Results clearly demonstrate that the east-west bias effect is largest over cloud free pixels, which strongly suggests that the problem is related to polarisation effects. Indeed additional investigations performed at DLR using the polarised radiative transfer code VLIDORT indicate that part of the observed effect can be explained by a polarisation dependence of the O_3 AMFs. However the full range of variation cannot be explained and it is likely that part of the observed viewing angle dependency is related to incorrect polarisation correction of the Level 1B data. This issue will be further studied in another VS project.

Table B.2. Cloud dependence (data 1 – 16 Sep 2007)

	O_3 VCD % diff	Residual % diff
All Pixels	-1.73	9.49
CF $\leq$ 0.2	-2.16	11.57
CF $\geq$ 0.6	-0.77	1.20

C. NO_2 COLUMN VERIFICATION

C.1. NO_2 slant column verification

For the NO_2 verification, the GDOAS and UPAS systems were synchronised using DOAS settings derived from experience with the ERS-2 GOME instrument. NO_2 slant columns are derived in the 425-450 nm interval. GOME-2 flight-model NO_2 absorption cross-sections have been implemented after checking their consistency with the GOME FM data. It was found that both data sets agree with each other to within a few percents.

In Figure C.1, NO_2 slant columns independently retrieved at BIRA-IASB using GDOAS, at DLR using UPAS and at IFE-Bremen (data provided by A. Richter) are compared. It is found that the three sets of slant columns agree very well, with a mean bias close to zero and a scatter of 8.8×10^{13} molec/cm^2, well below the typical uncertainty of NO_2 slant columns.

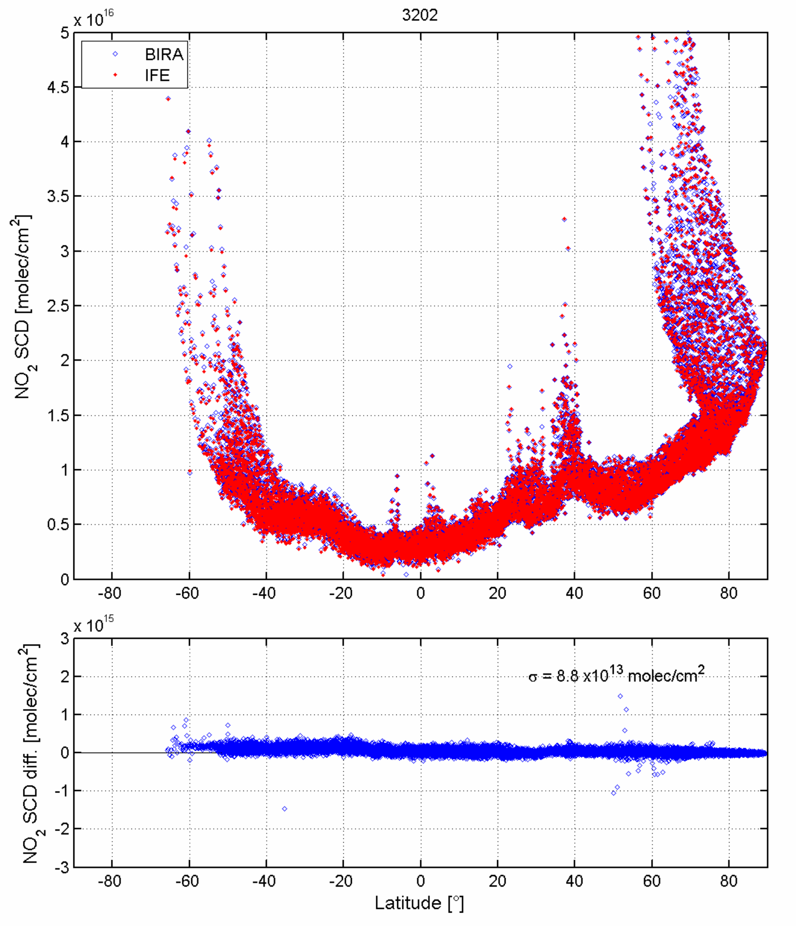

Figure C.1. Comparison between NO_2 slant columns retrieved using GDOAS, UPAS and the IFE-Bremen algorithm.

Further on, the consistency of the ERS-2 GOME and GOME-2 NO2 slant columns has been qualitatively investigated through the comparisons given in Figures C.2 and C.3. One can see that GOME-2 RMS fit residuals show typically larger variations. This behaviour has been attributed to the fact that GOME-2 measurements are limited by photon noise and not by undersampling effects. This means that GOME-2 NO_2 slant columns show reduced noise above bright scenes, such as produced by clouds.

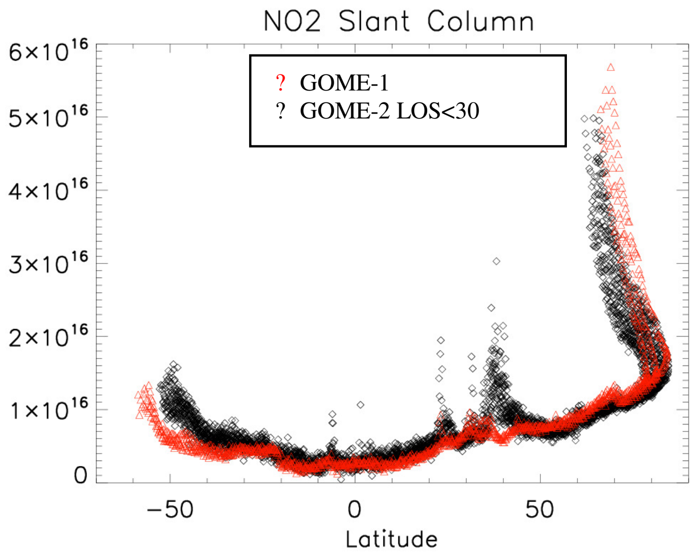

Figure C.2. Comparison between ERS-2 GOME and GOME-2 NO_2 slant columns, as retrieved from two sample orbits.

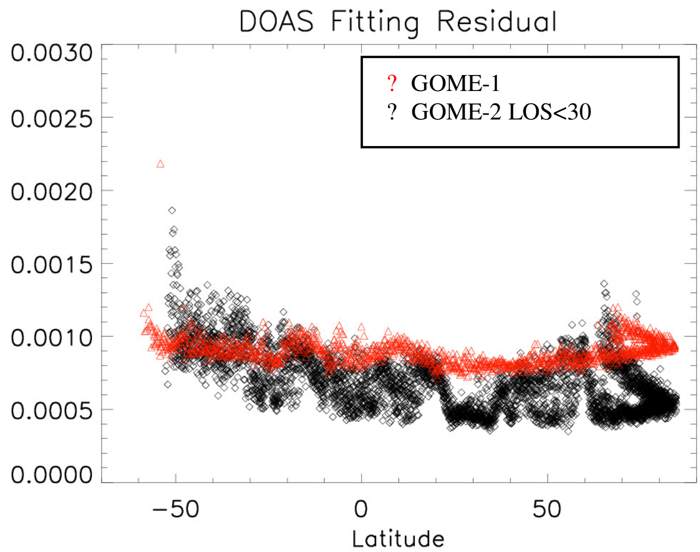

Figure C.3. Comparison of DOAS fit RMS residuals for NO_2 retrieval from two sample orbits from ERS-2 GOME and GOME-2. GOME-2 show smaller residuals than ERS-2 GOME over bright scenes.

C.2. Preliminary validation of NO_2 vertical columns

GOME-2 NO_2 vertical columns produced with the UPAS GDP 4.2 system have been compared to ground-based stratospheric column measurements from the NDACC network. In Figure C.4, the meridian structure of the NO_2 column differences between satellite and ground-based data sets is displayed, for the March-June 2007 period. As can be seen, there is an excellent qualitative agreement between GOME-2 and NDACC observations over this period, although GOME-2 GDP 4.2 seems to reports slightly smaller NO_2 vertical columns in the Southern hemisphere.

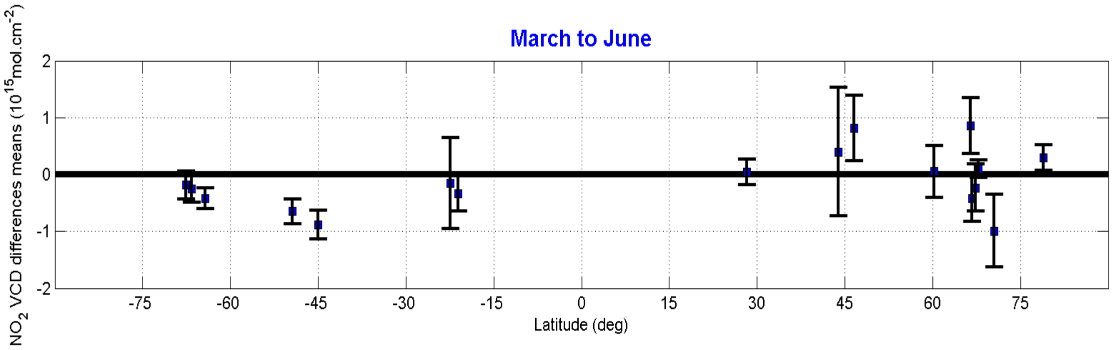

Figure C.4. Meridian structure of the NO2 column differences between GOME-2 GDP 4.2 and ground-based measurements from the NDACC.

In Figure C.5, the GDP 4.2 NO_2 columns are compared to SCIAMACHY NO2 columns generated within the TEMIS project (www.temis.nl). To simplify the interpretation of comparison results, both data sets were processed using simple geometrical air mass factors. As can be seen, results indicate an apparent underestimation of GOME-2 with respect to SCIAMACHY for the March-June period. The origin of this problem has been further investigated. It was found that the apparent difference between the two sensors was related to the way SCIAMACHY NO_2 columns are retrieved for TEMIS, i.e. using daily earthshine reference spectra combined with an equatorial normalisation approach. The latter method effectively assumes that the background NO_2 vertical columns can be considered as constant over the unpolluted equatorial Pacific region.

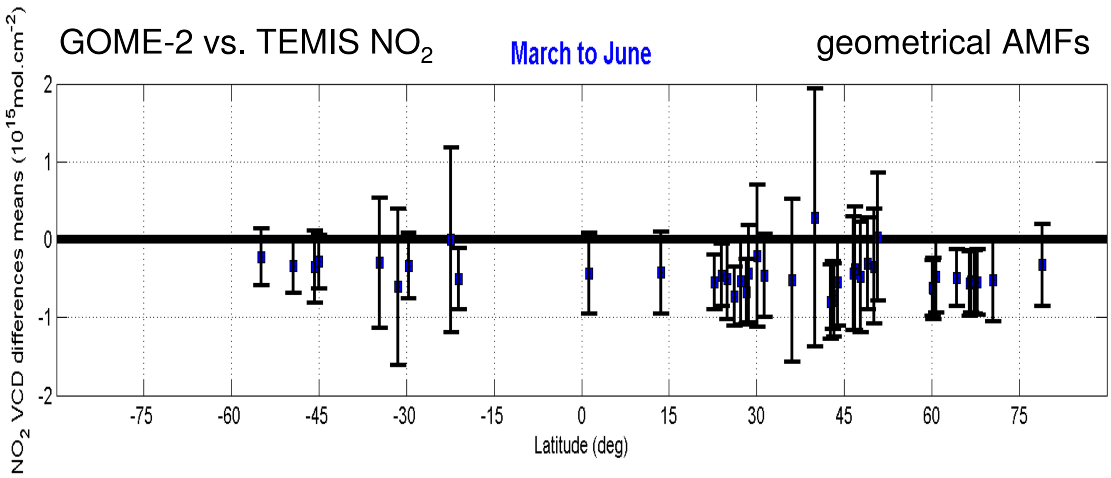

Figure C.5. Meridian structure of the NO_2 column differences between GOME-2 GDP 4.2 and the TEMIS NO_2 column product. To simplify the interpretation, geometrical AMF have been used in both cases.

Further retrieval exercises displayed in Figure C.6 show that, in contrast to the initial comparison results, GOME-2 and SCIAMACHY show highly consistent values when both data are processed in the same way, using as control spectrum the daily recorded solar irradiance spectrum. These results clearly indicate that background clean equatorial NO_2 column show significant variations (due dynamical effects such as QBO or semi-annual oscillation) that can be easily detected by the satellite measurements. When taking this into consideration, excellent agreement is found between GOME-2 and SCIAMACHY NO_2 retrievals.

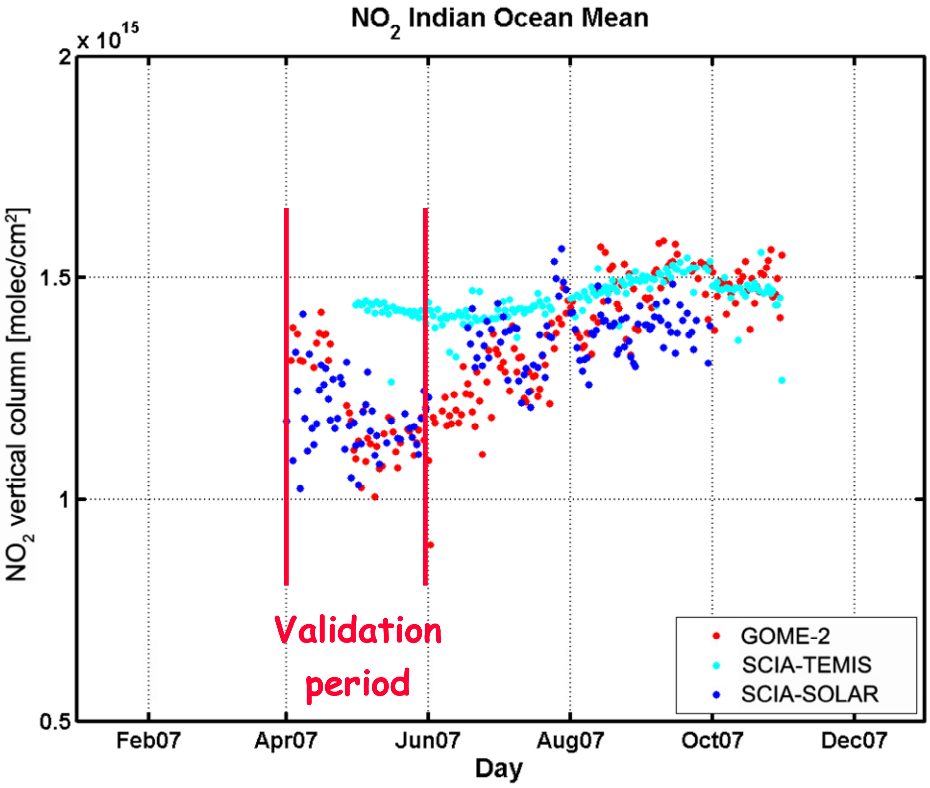

Figure C.6. Comparison between GOME-2 GDP 4.2 NO_2 column measurements and SCIAMACHY NO_2 columns retrieved using the equatorial normalisation approach (SCIA-TEMIS) and using a daily solar irradiance as reference spectrum (SCIA-SOLAR).

D. BRO COLUMN VERIFICATION

D.1. Settings for BrO column retrieval from GOME-2

D.1.1. Experience from ERS-2 GOME and SCIAMACHY

BrO columns have been retrieved from ERS-2 GOME and ENVISAT SCIAMACHY instruments and settings used for these two instruments are documented in the literature (e.g. Chance, 1998; Richter et al., 1998, 2002, Wagner and Platt, 1998; Van Roozendael et al., 1999, 2002, 2004; De Smedt et al., 2004). For the GOME instrument on ERS-2, BrO slant columns have been commonly derived in the wavelength interval from 344.7 to 359 nm, making use of the characteristic absorption structures of BrO in this region. This interval has been so far considered as optimal for BrO fitting from both satellite and ground-based observations (see e.g. Aliwell et al., 2002; Richter et al., 1998, 1999; Van Roozendael et al., 1998; Wagner and Platt, 1998) since spectral interferences with O_3, O_4, and HCHO are minimised in this region. In the case of SCIAMACHY however different settings had to be adopted, mainly due to the existence of strong polarisation features in the channel 2 of SCIAMACHY that cannot be eliminated by the polarization correction scheme implemented in the Level 0-1 processing. This polarization feature generates spurious interferences with the BrO spectral structures. To get rid of these polarization-related interferences, another fitting interval was adopted for SCIAMACHY displaced at shorter wavelengths in a region less affected by the polarization anomaly but still showing prominent BrO absorption features. It was shown that equally acceptable BrO columns could be retrieved from SCIAMACHY by including two absorption bands (336-347 nm) or three bands (336-351 nm). The SCIAMACHY BrO interval was generally found to produce BrO slant columns in good agreement with GOME (De Smedt et al., 2004; Van Roozendael et al., 2004), although a significant interference with HCHO absorption was noted. SCIAMACHY BrO maps also display systematic negative biases that correlate with orography, possibly due to unresolved spectral interferences with Ring or O_2-O_2.

D.1.2. Choice of BrO slant column settings for GOME-2

In an attempt to define a baseline for GOME-2 processing, the GOME and SCIAMACHY settings have been tested on GOME-2 spectra. As a result of the smaller pixel size of GOME-2 observations (approx. 40x80 km^2 instead of 40x320 km^2 for GOME) the noise on the individual GOME-2 BrO measurements was found to be significantly increased in comparison to GOME. On the basis of noise-driven considerations and test retrievals performed at DLR, the SCIAMACHY fitting interval using three absorptions bands (336 – 351.5 nm) was found to represent an optimal for GOME-2 retrieval and was selected for the generation of a first demonstration data set, which we now consider for evaluation. Although, as we said, the noise level was found to be significantly reduced in the 336-351.5 nm interval in comparison with the GOME baseline (344.7-359 nm), the comparison of BrO columns retrieved from GOME-2 in both spectral regions also revealed systematic differences, in particular a tendency to produce lower BrO slant columns at shorter wavelengths. This behaviour is illustrated in Figures D.1 and D.2 for one day in October 2007. In the absence of independent correlative measurements, it is difficult to determine whether one or the other of these retrieval options is satisfying. In the following the consistency of the GDP 4.2 BrO column demonstration product is investigated from the point of view of (1) the verification (i.e. whether BrO retrievals performed with GDP 4.2 are consistent with scientific retrievals performed using same settings), (2) the comparison against other satellite instruments (GOME and SCIAMACHY), and (3) the comparison against independent ground-based observations from two stations of the NDACC.

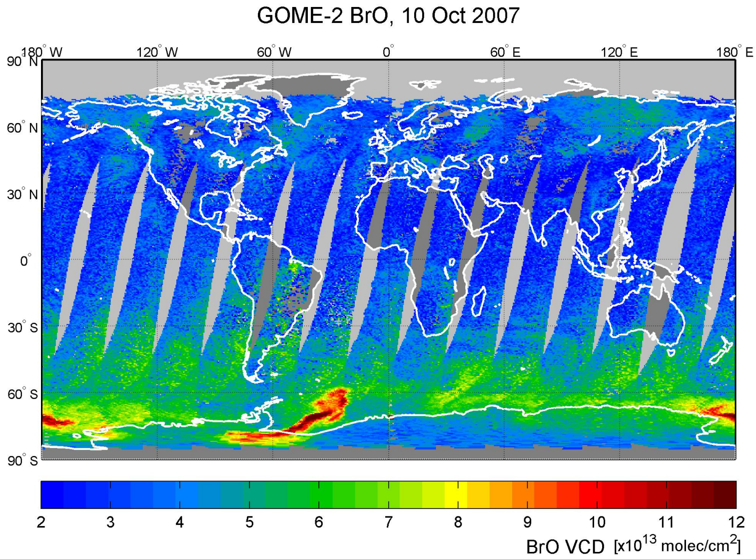

Figure D.1. BrO vertical columns derived from GOME-2 nadir radiances in the SCIAMACHY fitting interval (336 - 351.5 nm). Geometrical air mass factors have been used for the slant to vertical column conversion.

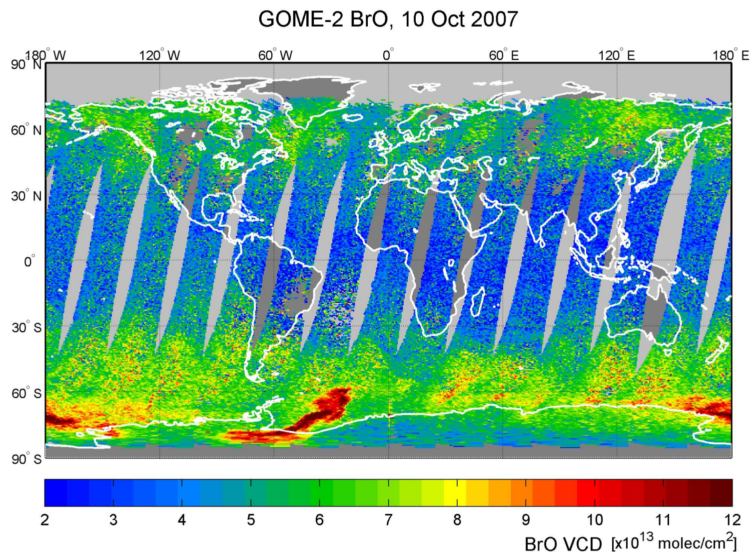

Figure D.2. BrO vertical columns derived from GOME-2 nadir radiances in the ERS-2 GOME fitting interval (344.7 - 359 nm). Geometrical air mass factors have been used for the slant to vertical column conversion.

D.2. Verification of BrO slant columns and sensitivity tests

For verification purposes, the retrieval software of BIRA-IASB was synchronised with the GDP 4.2 processor, using a common set of slant column retrieval settings, as documented in Table D.1. Comparisons between the two processing systems were performed on a limited set of GOME-2 orbits. Results of the se comparisons are illustrated in Figures D.3 and D.4. Clearly a high level of agreement was obtained, demonstrating the consistency between the two slant column fitting algorithms.

Table D.1. DOAS settings used for GOME-2 BrO slant column verification

Fitting interval	336 – 351.5 nm
Sun reference	Sun irradiance from file
Wavelength calibration	Wavelength calibration of sun reference optimized by NLLS adjustment on convolved Chance and Spurr solar lines atlas
Absorption cross-sections	
- BrO	Fleischmann et al., 223°K (2004)
- NO_2	GOME FM3, 243°K
- Ozone	GOME FM98 smoothed at GOME-2 resolution, 221°K + 241°K
- O_2-O_2	Greenblatt et al. (1990); wavelength axis corrected by Burkholder
- Ring effect	2 Ring eigenvectors generated using SCIATRAN
Polynomial	3rd order (4 parameters)
Intensity offset correction	Constant offset

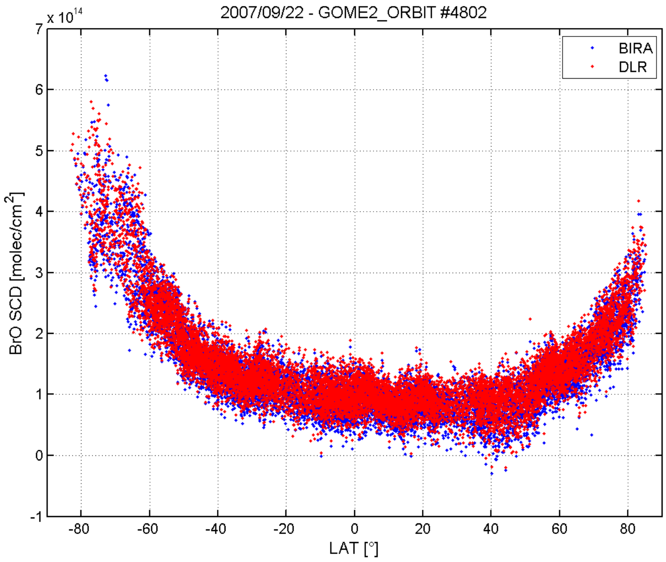

Figure D.3. Comparison of BrO slant columns retrieved from GDP 4.2 and from the BIRA-IASB scientific algorithm. DOAS settings were synchronised according to Table D.1.

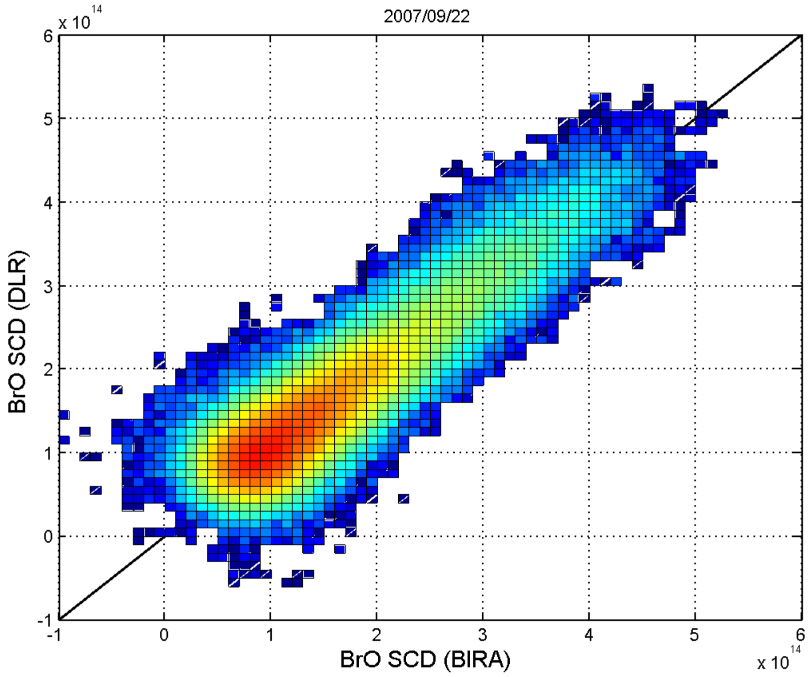

Figure D.4. Correlation plot of BrO slant columns retrieved from GDP 4.2 and the BIRA-IASB scientific algorithm. All GOME-2 orbits from 22 September 2007 are considered.

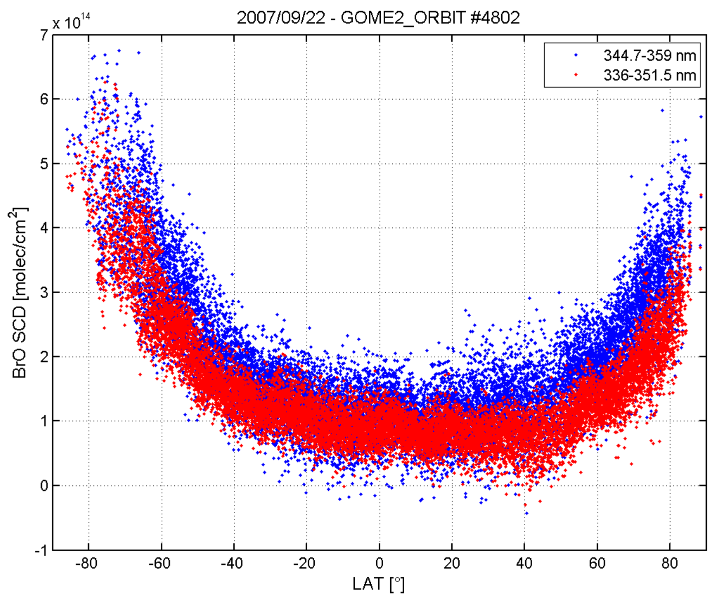

Figure D.5. Comparison of BrO slant columns (SCDs) retrieved from GOME-2 in both GOME and SCIAMACHY fitting intervals. The scatter is larger in the GOME interval, but the average BrO SCD values are also larger, especially in the Northern hemisphere.

The sensitivity of the BrO slant column retrieval was further investigated by comparing GOME-2 evaluations in SCIAMACHY and GOME intervals both retrieved using the BIRA-IASB algorithm. In Figure D.5, the orbit selected for verification has been processed in both intervals. As previously mentioned results show a tendency to produce higher columns in the GOME interval. Such differences are systematic as can be seen from monthly averaged plots of BrO column inverted from both fitting ranges (Figures D.6 and D.7). Note that at least for the period investigated here the differences tend to be larger in average in the Northern hemisphere than in the Southern hemisphere, as can be seen from statistics given in Table D.2. The well-known HCHO interference characteristic of the SCIAMACHY fitting interval is also clearly visible in Figure D.7, especially over regions of biomass burning like Brazil or Central Africa.

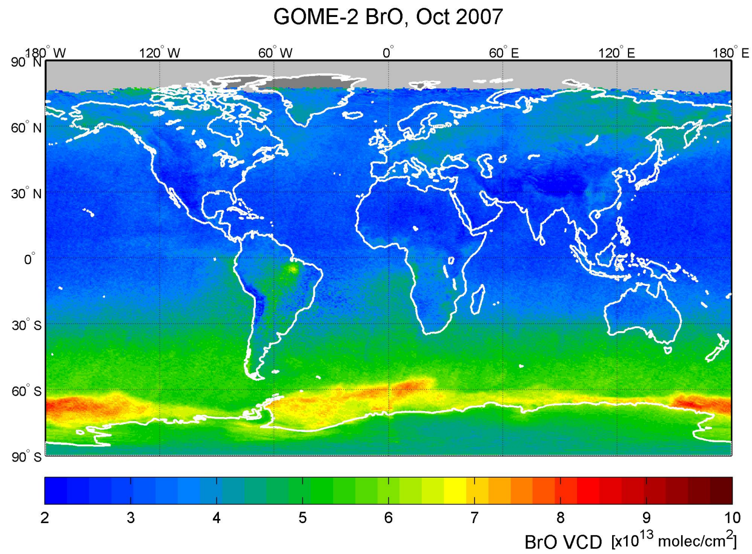

Figure D.6. Monthly average of GOME-2 BrO VCDs retrieved for October 2007 in the fitting interval 336 - 351.5 nm. Geometrical air mass factors have been used for the slant to vertical column conversion.

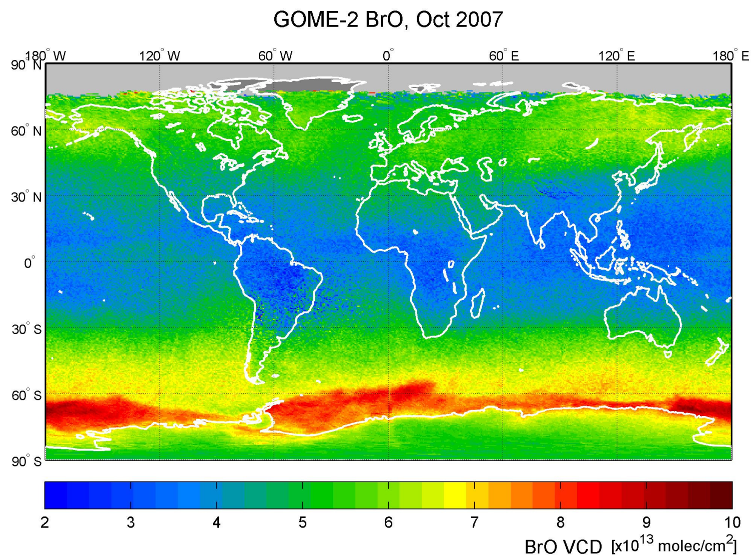

Figure D.7. Monthly average of GOME-2 BrO VCDs retrieved for October 2007 in the fitting interval 344.7 - 359 nm. Geometrical air mass factors have been used for the slant to vertical column conversion.

Table D.2. Statistical analysis of the differences in BrO SCDs retrieved from the GOME and SCIAMACHY fitting interval, for the GOME-2 orbit represented in Figure D.5.

Latitude band	Mean dev. [molec/cm^2]	Std. [molec/cm^2]	Std of the mean [molec/cm^2]	Mean Dev. [%]
60°N - 90°N	-8.2	7.3	0.18	-29
30°N - 60°N	-5.7	13.2	0.29	-29
30°S – 30°N	-2.0	3.9	0.06	5.6
30°S – 60°S	-4.4	4.3	0.08	-18
60°S – 90°S	-5.6	5.5	0.22	-13
All latitudes	-4.3	7.5	0.07	-12

D.3. Comparison against satellite data

BrO slant and vertical column amounts derived from the GOME and SCIAMACHY instruments have been produced at BIRA-IASB as part of the DUP/DUE TEMIS service (www.temis.nl). These data sets are been used here for comparison with GOME-2 retrievals from the GDP 4.2 demonstration data set. In order to simplify the comparison process within the limited timeframe available for this study, we based our analysis on overpass files extracted by the DLR team for a number of ground-based correlative sites, as detailed in Table D.3.

Table D.3. List of overpass sites used for the comparison with GOME and SCIAMACHY

Station	Latitude [°]	Longitude [°]	Altitude [m]
Ny_Alesund	78.92	11.92	8
Scoresbysund	70.48	-21.97	17
Sodankyla	67.37	26.65	179
Salekhard	66.67	66.67	0
Jokioinen	60.82	23.48	103
Helsinki	60.32	24.97	56
Harestua	60.20	10.80	580
St_Petersburg	59.97	30.30	60
Zvenigorod	55.68	36.77	200
Hamburg	53.57	9.97	105
Leicester	52.62	-1.12	90
De_Bilt	52.10	5.18	15
Cabauw	51.97	4.93	10
Paris	48.85	2.35	50
Verrieres_Le_Buisson	48.76	2.24	0
Jungfraujoch	46.55	7.98	3450
Haute.Provence	43.91	5.75	580
Issyk Kul	42.62	76.97	1640
Thessaloniki	40.63	22.96	60
XiangHe	39.75	116.96	36
GSFC	38.99	-76.84	102
Table_Mountain	34.38	-117.68	2200
Sevilleta	34.35	-106.88	1477
Kanpur	26.45	80.35	142
Mussafa	24.37	54.47	10
Mukdahan	16.61	104.68	166
Djougou	9.71	1.68	430
Ilorin	8.32	4.34	350
Merida	8.24	-71.08	4765

Nairobi	-1.32	36.92	1624
La Reunion	-21.06	55.48	24
Sao_Paulo	-23.56	-46.73	865
Kerguelen	-49.35	70.25	2
Dumont_D'Urville	-66.67	140.02	40

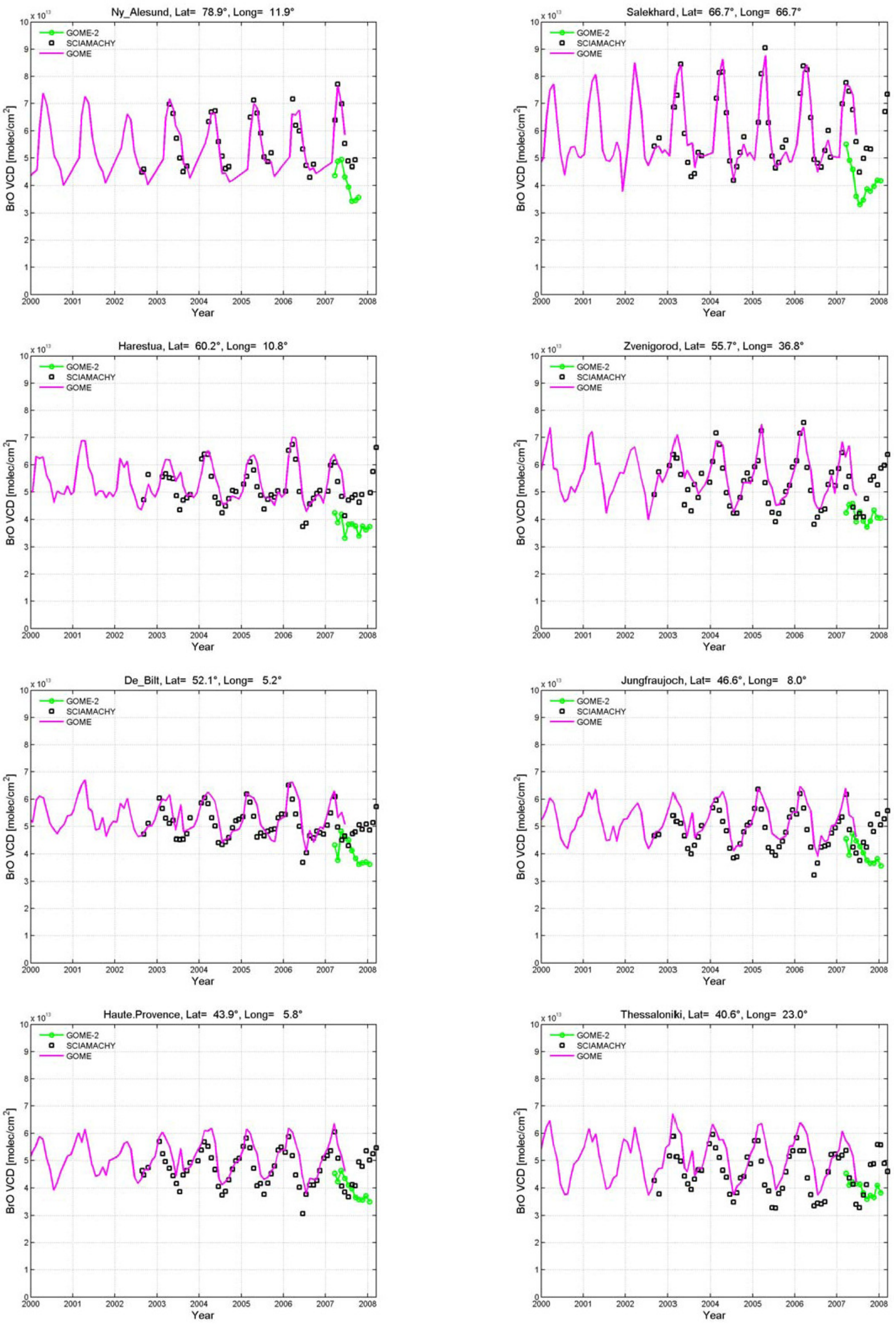

Figure D.8. Comparison of time-series of monthly averaged BrO vertical columns retrieved from ERS-2 GOME, SCIAMACHY and GOME-2 over the 2000-2008 period, at a number of ground-based sites.

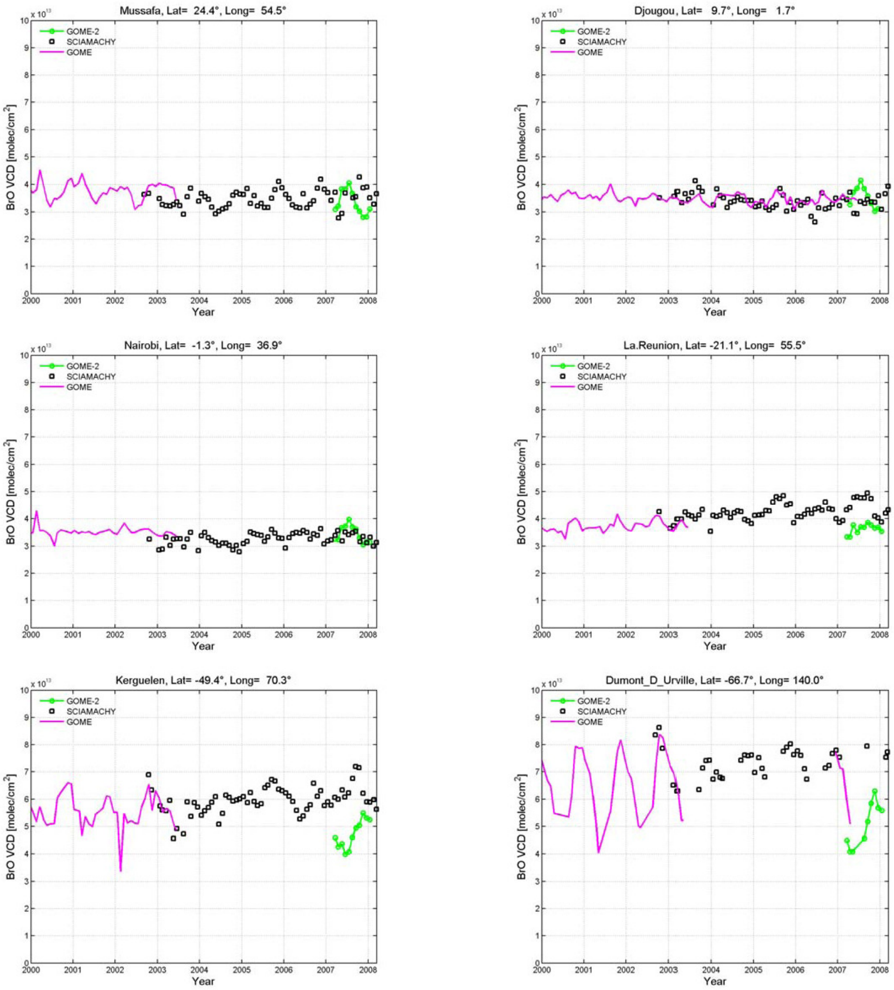

Figure D.8. Continued.

GOME-2, SCIAMACHY and GOME BrO columns have been extracted above each site according to measurement periods available from the different data sets. In order to provide a meaningful temporal perspective, time-series of monthly averaged BrO columns have been plotted for comparison over the time period from 2000 until 2008. In the case of GOME and SCIAMACHY, simple geometrical AMFs were used for the slant to vertical column conversions. Although BrO AMFs used in the GDP 4.2 environment were generated using the LIDORT radiative transfer code, these were calculated for pure stratospheric BrO profiles. It was verified that under these conditions, the GDP 4.2 AMFs are close to geometrical AMFs within a few percents. Results from the GOME, SCIAMACHY and GOME-2 comparisons are represented in Figure D.8 for a representative selection of sites.

As can be seen, the GOME-2 BrO vertical columns are generally smaller than those retrieved from GOME and SCIAMACHY at high latitude sites of both hemispheres. At mid-latitudes and in the tropics, the general agreement is better overall although the winter maximum at mid-latitude is generally smaller as well. In the tropics and equatorial belts, the average level is highly consistent for all three data sets. One exception is Reunion Island. At this site however the SCIAMACHY columns are affected by a suspicious positive trend, and must therefore be treated with caution. For some tropical sites (e.g. Mussafa) the seasonal patterns also seem to be differently documented by GOME-2 retrievals.

In Figure D.9, all coincident monthly average BrO VCD values are compared in a correlation plot. The column-dependency of the differences reaches 30 percents for the largest columns, as can be also seen in Figure D.10 where relative differences are expressed as a function of the BrO VCD.

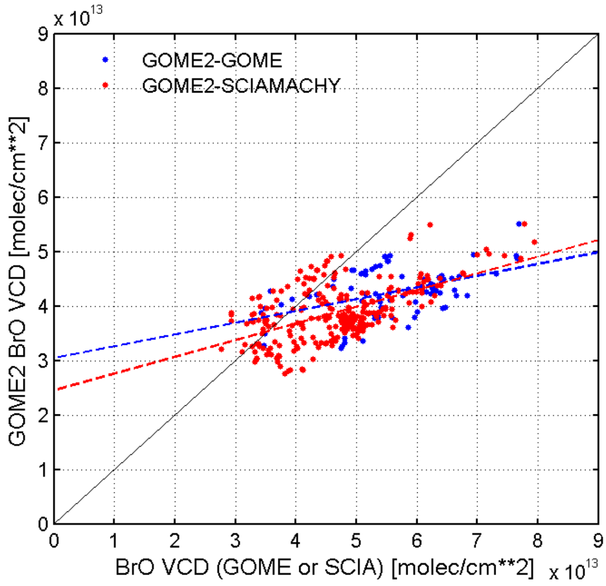

Figure D.9. Correlation between BrO VCD retrieved from GOME-2 and, respectively, GOME and SCIAMACHY. The solid line represents the reference line of slope equal to unity.

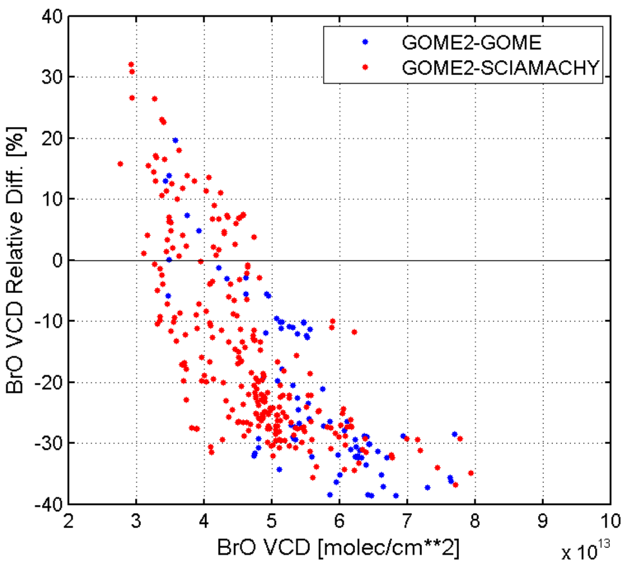

Figure D.10. Relative differences in BrO VCD between GOME-2 and, respectively, GOME and SCIAMACHY, plotted as a function of the reference BrO VCD (GOME or SCIAMACHY).

D.4. Comparison against ground-based measurements

Ground-based zenith-sky UV-visible observations have been continuously performed at the NDACC station of Harestua, Norway since 1998 as well as in Lauder, New-Zealand since 1995. The instruments consist of zenith-sky looking grating spectrometers using cooled photodiode-array detectors. Spectral range and resolution are optimised for BrO measurements in the 330–360 nm. Total, stratospheric and tropospheric BrO columns are retrieved from measured slant columns using a profiling algorithm based on the optimal estimation method, as described in Hendrick et al. (2007). The sensitivity of the zenith-sky observations to the tropospheric BrO detection is increased by using for the spectral analysis a fixed reference spectrum corresponding to clear-sky noon summer conditions. The use of a photochemical box-model optimised for bromine chemistry embedded inside the inversion tool allows performing retrievals at any solar zenith angle, therefore allowing for appropriate photochemical matching with satellite observations.

In order to provide an independent reference, BrO total columns derived from latest versions of the ground-based measurements have been compared to GDP 4.2 BrO columns for the period from summer 2007 until autumn 2008. Results, displayed in Figure D.11, show good agreement with GOME-2 baseline retrievals in the 336-351.5 nm interval. These results are in contrast with those reported in a previous note (ref: TN-IASB-GOME2-O3MSAF-BrO-01-ORR-A3) and reflect progress recently made in the evaluation of ground-based measurements now available at an increasing number of sites. They also raise questions about the accuracy of the previously retrieved GOME and SCIAMACHY data products, which were used as an input to the comparisons presented in section D.3. This issue is addressed in the next section.

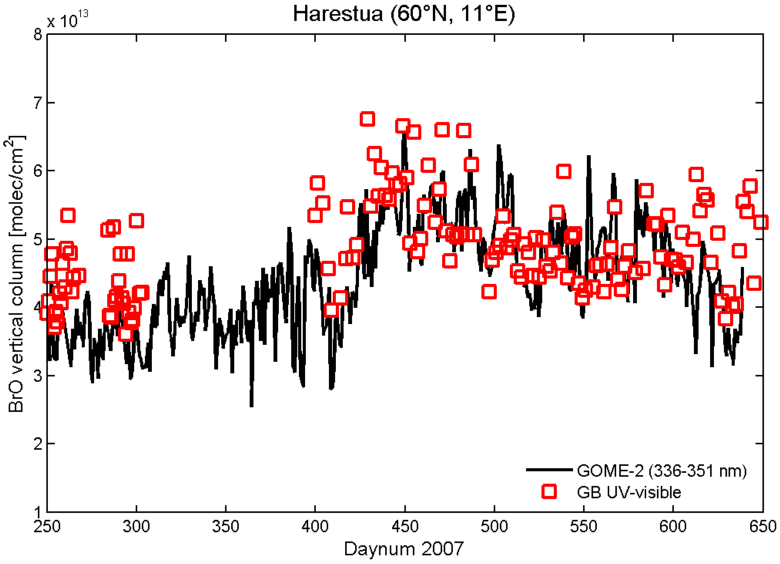

Figure D.11. Comparison of BrO total columns derived from GOME-2 in the baseline interval 336-351.5 nm and from ground-based UV-visible measurements at the Harestua station (data originators: F. Hendrick and M. Van Roozendael).

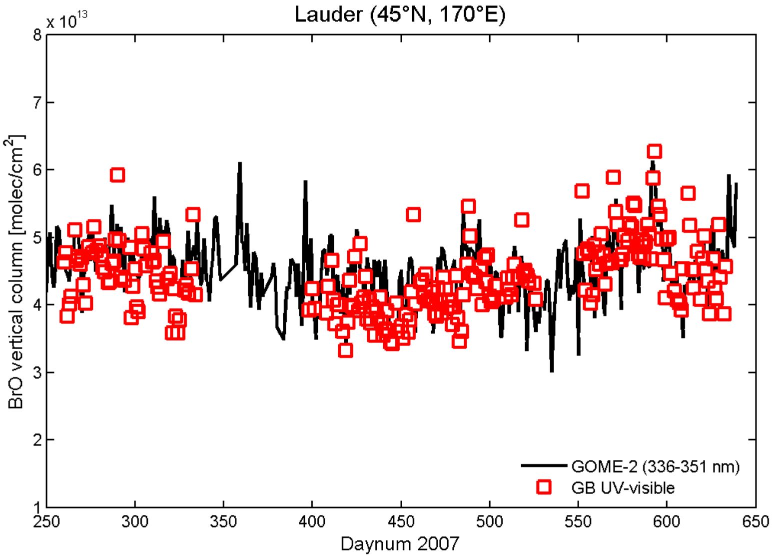

Figure D.11. Comparison of BrO total columns derived from GOME-2 in the baseline interval 336-351.5 nm and from ground-based UV-visible measurements at the Lauder station (data originators: Paul Johnston and F. Hendrick).

D.5. Sensitivity of GOME-2 BrO retrievals to DOAS settings changes

Ground-based validation results presented in the previous section suggest that GOME-2 (and ERS-2 GOME) BrO slant columns tend to be overestimated when retrieved in the "traditional" GOME interval 345-359 nm. In order to further investigate the possible reasons of this overestimation in an attempt to reconcile BrO retrievals in both intervals, a series of sensitivity tests have been performed. DOAS settings were varied in both intervals and the stability of the BrO slant columns was investigated. It was found that the retrieved BrO slant columns are a lot more stable in the shorter wavelength interval, as illustrated in Figure D.12.

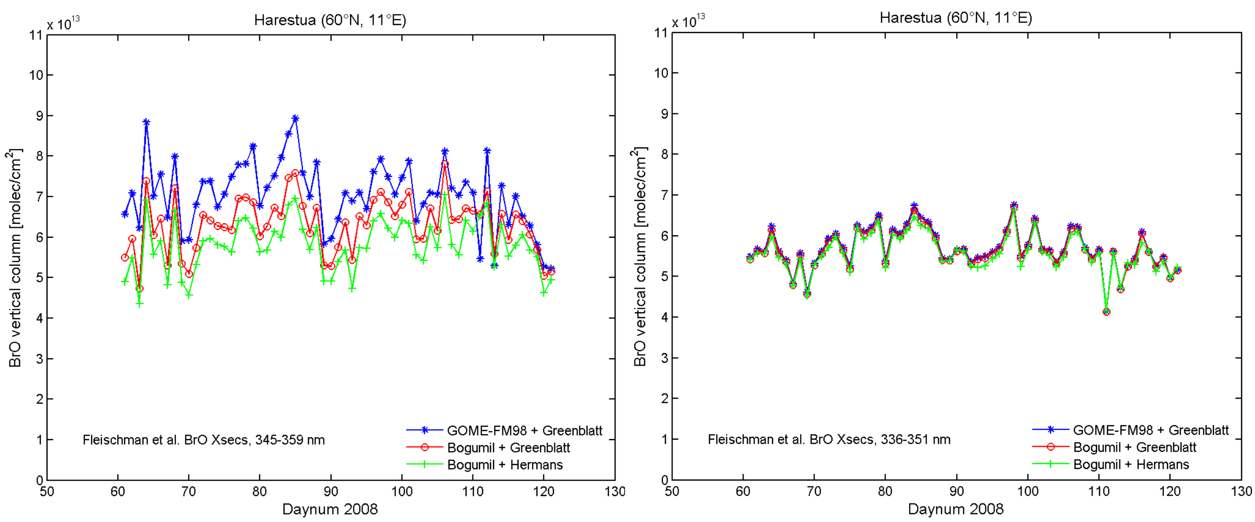

Figure D.12. Comparison of BrO columns retrieved in the 345-359 nm interval (left hand panel) and in the 336-351.5 nm interval (right hand panel), using different choices of reference O_3 and O_4 absorption cross-sections.

In particular it was found that in the longer wavelength range, BrO slant columns are highly sensitive to the choice of the reference laboratory cross-sections of both O_3 and O_4. According to our tests, a switch from our past baseline (O_3 cross-sections from Burrows et al., 1999 and O_4 cross-sections from Greenblatt et al., 1990) to an alternative choice of laboratory measurements, i.e. O_3 cross-sections from Bogumil et al. (1999) and O_4 cross-sections from Hermans et al. (http://www.aeronomie.be/spectrolab/o2.htm) leads to significantly smaller BrO columns in better agreement with results obtained in the 336-351.5 nm interval, while residuals are only weakly modified. These results are similarly illustrated by color plots displayed in Figures D.13 and D.14.

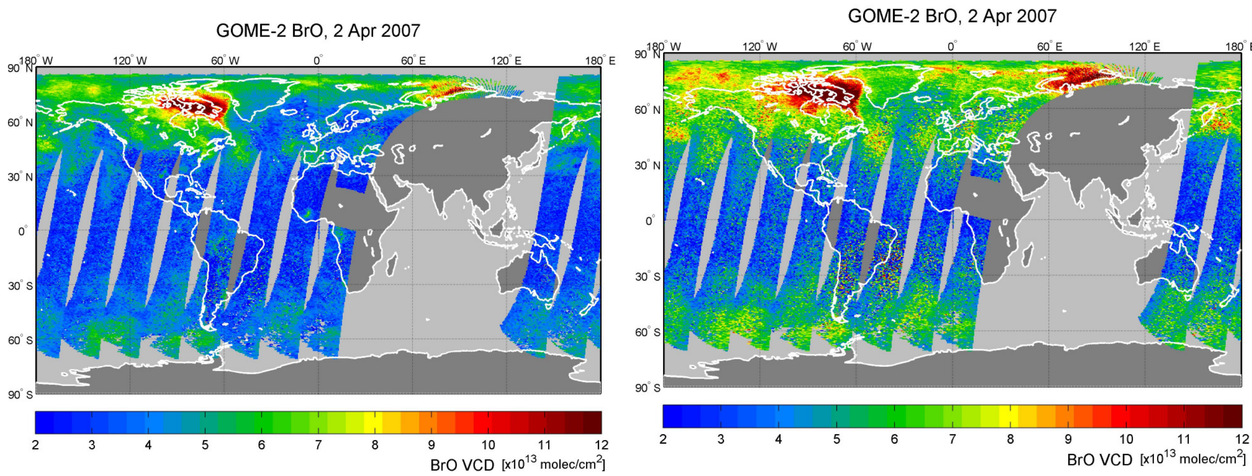

Figure D.13. Comparison of BrO columns retrieved in the 336-351.5 nm interval (left hand panel) and in the 345-359 nm interval (right hand panel), using O_3 absorption cross-sections from Burrows et al. (1999, GOME FM98) and O_4 cross-sections from Greenblatt et al. (1990).

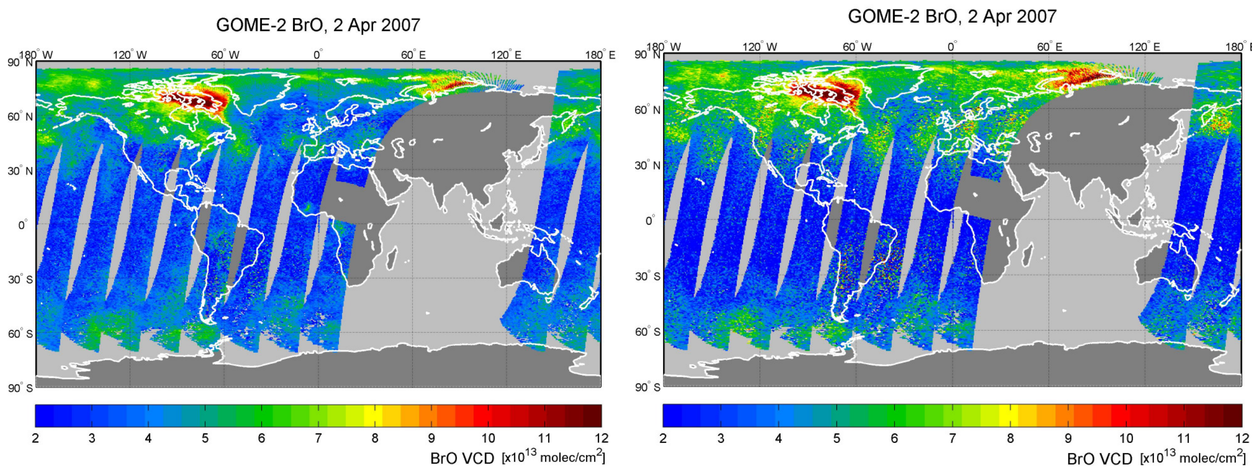

Figure D.14. Comparison of BrO columns retrieved in the 336-351.5 nm interval (left hand panel) and in the 345-359 nm interval (right hand panel), using O_3 absorption cross-sections from Bogumil et al. (1999) and O_4 cross-sections from Hermans et al. (http://www.aeronomie.be/spectrolab/o2.htm)

For completeness, the inconsistency reported in section D.2. between GOME-2 and SCIAMACHY BrO slant columns has been investigated as well. In this case, both data sets are retrieved in the same wavelength interval (336-351 nm). Although instrument-specific bias might have been suspected, the problem could actually be easily tracked as being due to the use of the outdated BrO cross-section from Wahner et al. (1988) for the SCIAMACHY retrieval. These cross-sections suffer from inadequate spectral resolution, which results in a systematic overestimation of the BrO slant columns by approximately 20 %. Switching the SCIAMACHY retrievals to the Fleischmann et al. (2004) BrO cross-sections data set in use for GOME-2 largely resolves the apparent inconsistency.

E. CONCLUSIONS

As part of this visiting scientist project, the verification of GOME-2 total ozone, NO_2 and BrO products has been addressed, based on tools available at BIRA-IASB.

For total ozone, GDOAS and GDP 4.2 have been found to be consistent within approximately 1 %, with main differences being due to different cloud product in the scientific and operational processing systems. The east-west pixel anomaly in total ozone reported by P. Valks and the DLR team has been confirmed by scientific retrievals. An analysis of the cloud dependence of the bias strongly suggests that it is related to a polarization issue.

Regarding NO_2, the verification of slant columns concludes to an excellent consistency between the operational data products and scientific evaluations performed at BIRA-IASB and IFE-Bremen. Initial NDACC-based validation suggests a possible negative bias in Southern hemisphere, while excellent agreement is found with SCIAMACHY when considering satellite evaluations consistently performed using solar irradiances as control spectra.

GOME-2 BrO vertical columns have been evaluated using (1) scientific retrievals based on the GDOAS tool and (2) comparisons with correlative data sets from SCIAMACHY and GOME and from ground-based zenith-sky measurements. The fitting interval 336-351.5 nm previously used for SCIAMACHY retrievals has been selected as baseline for BrO slant column retrieval in GDP 4.2. This interval has been found to minimise the noise on the GOME-2 BrO columns, however a systematic bias low with respect to test retrievals performed in the traditional GOME interval (344.7-359 nm) was also identified.

For verification purpose, the GDOAS and GDP 4.2 retrieval tools were synchronised until a satisfying level of agreement was found confirming the reliability of the GDP for BrO slant column fitting. However further comparisons with GOME and SCIAMACHY data reveal some inconsistencies, GOME-2 reporting smaller BrO columns than other sensors. The bias is found to be largest a high latitude reaching -30 % in average for BrO columns larger than $5x10^{13}$ molec/cm^2.

Additional comparisons using latest versions of available ground-based DOAS measurements at two stations of the NDACC (Harestua, Norway and Lauder, New Zealand) do not confirm these findings but instead consolidate the GOME-2 retrievals. In order to resolve the apparent inconsistency between ERS-2 GOME and GOME-2, additional sensitivity tests have been performed to explore the stability of BrO slant column fit results in both fitting ranges. It is found that retrievals in the longer wavelength range (previously used for GOME) are more sensitive to uncertainties in O_3 and O_4 absorption cross-sections. Using an alternative combination of reference spectra (Bogumil et al., 1999 for O_3 and Hermans et al., for O_4) the BrO slant columns can be brought to similar values in both fitting ranges. The stability of the DOAS fits in the 336-351.5 nm wavelength region provides further evidence of the reliability of these retrievals. Note however that the known interference between spectral signatures of BrO and HCHO, already identified in SCIAMACHY, still result in BrO columns being positively biased over regions of large HCHO emissions (e.g. central Africa, southern America or eastern China).

For longer term validation, the currently expanding ground-based BrO monitoring capabilities will be further exploited. In particular the growing interest for the study of polar bromine emissions will lead to extension of ground-based MAXDOAS networks in polar regions.

F. REFERENCES

F.1. Peer-reviewed articles and conference proceedings

Aliwell, S. R., M. Van Roozendael, P. V. Johnston, A. Richter, T. Wagner, D. W. Arlander, J. P. Burrows, D. J. Fish, R. L. Jones, K. K. Tørnkvist, J.-C. Lambert, K. Pfeilsticker, and I. Pundt, Analysis for BrO in zenith-sky spectra: An intercomparison exercise for analysis improvement, J. Geophys. Res., 107, D14, doi: 10.1029/2001JD000329, 2002

Bass, A.M., and R.J. Paur, The Ultraviolet Cross-Sections of Ozone, I, The Measurements, in: Atmospheric Ozone, edited by C. S. Zerefos and A. Ghazi, pp. 606-610, D. Reidel, Norwell, Mass., 1985.

Bogumil, K. , J. Orphal, S. Voigt, H. Bovensmann, O. C. Fleischmann, M. Hartmann, T. Homann, P. Spietz, and J. P. Burrows, Reference spectra of atmospheric trace gases measured with the SCIAMACHY PFM satellite spectrometer. In ESAMS '99 - European Symposium on atmospheric Measurements from Space, volume 2, pages 443–447, 1999.

Brion, J., Chakir, A., Charbonnier, J., Daumont, D., Parisse, C. and Malicet, J., Absorption spectra measurements for the ozone molecule in the 350-830 nm region, J. Atmos. Chem., 30, 291-299, 1998.

Brion, J., Chakir, A., Daumont, D. and Malicet, J., High-resolution laboratory absorption cross section of O3. Temperature effect, Chem. Phys. Lett., 213 (5-6), 610-512, 1993.

Burrows, J.P., A. Richter, A. Dehn, B. Deters, S. Himmelmann, S. Voigt, and J. Orphal, Atmospheric Remote-Sensing Reference Data from GOME: 2. Temperature-Dependent Absorption Cross Sections of O_3 in the 231-794 nm Range, J. Quant. Spectrosc. Rad. Transf. 61, 509-517, 1999.

Chance, K., Analysis of BrO measurements from the Global Ozone Monitoring Experiment, Geophys. Res. Lett., 25, 3335-3338, 1998.

Daumont, M., Brion, J., Charbonnier, J. and Malicet, J., Ozone UV spectroscopy I: Absorption cross-sections at room temperature, J. Atmos. Chem., 15, 145-155, 1992.

Fietkau, S., T. Medeke, A. Richter, N. Sheode, B.-M. Sinnhuber, F. Wittrock, N. Theys, M. Van Roozendael and J.P. Burrows, Comparison of ground-based measurements and model calculations of bromine Monoxide above Nairobi (1°S, 36°E), submitted to Atmos. Chem. Phys. (2007)

Fitzenberger, R., Bösch, R., Camy-Peyret, C., Chipperfiel, M.P.,Harder, H., Platt, U., Sinnhuber, B.-M., Wagner, T., and Pfeilsticker, K.: First profile measurements of tropospheric BrO, Geophys. Res. Lett., 27, 2921-2924, 2000.

Fleischmann, O. C., Hartmann, M., Burrows J. P., and Orphal, J.: New ultraviolet absorption cross-sections of BrO at atmospheric temperatures measured by time-windowing Fourier transform spectroscopy, J. Photochem. Photobiol. A, 168, 117–132 , 2004.

Greenblatt, G. D., J. J. Orlando, J. B. Burkholder, and A. R. Ravishankara, Absorption measurements of oxygen between 330 and 1140 nm. J. Geophys. Res., 95, 18 577–18 582, 1990.

Hendrick, F., M. Van Roozendael, M. P. Chipperfield, M. Dorf, F. Goutail, X. Yang, C. Fayt, C. Hermans, K. Pfeilsticker, J.-P. Pommereau, J. A. Pyle, N. Theys, and M. De Mazière, Retrieval of stratospheric and tropospheric BrO profiles and columns using ground-based zenith-sky DOAS observations at Harestua, 60°N, Atmos. Chem. Phys., 7, 4869–4885, 2007.

Hendrick, F., P.V. Johnston, K. Kreher, C. Hermans, M. De Mazière, and M. Van Roozendael, One decade trend analysis of stratospheric BrO over Harestua (60°N) and Lauder (44°S) reveals a decline, submitted to Geophys. Res. Lett. (2008).

Malicet, C., Daumont, D., Charbonnier, J., Parisse, C., Chakir, A. and Brion, J.: Ozone UV spectroscopy, II.

Paur, R.J., and A.M. Bass, The Ultraviolet Cross-Sections of Ozone, II, Results and Temperature Dependence, in: Atmospheric Ozone, edited by C. S. Zerefos and A. Ghazi, pp. 611-616, D. Reidel, Norwell, Mass., 1985.

Pundt, I., J.-P. Pommereau, M.P. Chipperfield, M. Van Roozendael, and F. Goutail, Climatology of the stratospheric BrO vertical distribution by balloon borne UV-Vis spectroscopy, J. Geophys. Res., 107, doi: 10.1029/2002JD002230, 2002.

Richter, A., Eisinger, M., Ladstätter-Weissenmayer, A., and Burrows, J.P.: DOAS zenith-sky observations, 2, seasonal variation of BrO over Bremen (53°N) 1994-1995, J. Atmos. Chem., 32, 83-99, 1999.
Richter, A., Wittrock, F., Eisinger, M., and Burrows, J. P.: GOME observations of tropospheric BrO in Northern Hemispheric spring and summer 1997, Geophys. Res. Lett., 25, 2683-2686, 1998.
Richter, A., Wittrock, F., Ladstätter-Weissenmayer, A., and Burrows, J. P.: GOME measurements of stratospheric and tropospheric BrO, Adv. Space Res., 29, 1667-1672, 2002.
Theys, N., I. De Smedt, C. Fayt, M. Chipperfield, P. Post, R. van der A, and M. Van Roozendael, Total and tropospheric BrO derived from GOME and SCIAMACHY as part of the TEMIS project, in Proc. of the ERS/ENVISAT 2004 Symposium, Salzburg, Austria, 6 – 10 September, 2004.
Theys, N., M. Van Roozendael, F. Hendrick, C. Fayt, C. Hermans, J.-L. Barray, F. Goutail, J.-P. Pommereau and M. De Mazière, Retrieval of stratospheric and tropospheric BrO columns from multi-axis DOAS measurements at Reunion Island (21°S, 56°E), Atmos. Chem. Phys., 7, 4733–4749, 2007.
Theys, N., M. Van Roozendael, Q. Errera, S. Chabrillat, F. Daerden, F. Hendrick, D. Loyola, P. Valks, A Stratospheric BrO Climatology Based on the BASCOE 3D Chemical Transport Model, in Proceedings of the ENVISAT Symposium 2007, Montreux, Switzerland, 23-27 April, ESA publication SP-636, 2007.
Van Roozendael, M., I. De Smedt, C. Fayt, F. Wittrock, A. Richter, O. Afe, First validation of SCIAMACHY BrO columns, in Proc. Second Workshop on the Atmospheric Chemistry Validation of ENVISAT (ACVE-2), Frascati, Italy, 3 – 7 May, 2004.
Van Roozendael, M., A. Richter, T. Wagner, I. Pundt, D. W. Arlander, J. P. Burrows, M. Chipperfield, C. Fayt, P. V. Johnston, J.-C. Lambert, K. Kreher, K. Pfeilsticker, U. Platt, J.-P. Pommereau, B.-M. Sinnhuber, K. K. Tørnkvist, and F. Wittrock, Intercomparison of BrO Measurements From ERS-2 GOME, Ground-Based and Balloon Platforms, Adv. Space Res., 29, 1661-1666, 2002.
Van Roozendael, M., C. Fayt, J.-C. Lambert, I. Pundt, T. Wagner, A. Richter, and K. Chance, Development of a bromine oxide product from GOME, Proc. ESAMS'99-European Symposium on Atmospheric Measurements from Space, ESTEC, Noordwijk, The Netherlands, 18-22 January 1999, WPP-161, p. 543-547, 1999.
Van Roozendael, M., Fayt, C., Hermans, C., and Lambert, J.-C., Ground-based UV-visible Measurements of BrO, NO_2, O_3 and OClO at Harestua (60° N) since 1994, Proceedings of the 4th European Workshop on Polar Stratospheric Ozone, Schliersee, Germany, 22–26 Sept 1997, Air Pollution Research Report no 66, European Commission – DG XII, Brussels, 1998.
Van Roozendael, M., N. Theys, F. Hendrick, Total and tropospheric BrO retrieval from space-nadir and ground-based UV-Vis observations, a contribution to sub-project ACCENT-TROPOSAT-2 (AT2), Task Group 1, AT2 Annual Report 2005-2006, 2006.
Vandaele, A.C., C. Fayt, F. Hendrick, C. Hermans, F. Humbled, M. Van Roozendael, M. Gil, M. Navarro, O. Puentedura, M. Yela, G. Braathen, K. Stebel, K. Tørnkvist, P. Johnston, K. Kreher, F. Goutail, A. Mieville, J.-P. Pommereau, S. Khaikine, A. Richter, H. Oetjen, F. Wittrock, S. Bugarski, U. Friess, K. Pfeilsticker, R. Sinreich, T. Wagner, G. Corlett, R. Leigh, An intercomparison campaign of ground-based UV-Visible measurements of NO_2, BrO, and OClO slant columns. I. Methods of analysis and results for NO2, J. Geophys. Res., 110, D08305, doi:10.1029/2004JD005423, 2005.
Wagner, T., and Platt, U.: Satellite mapping of enhanced BrO concentrations in the troposphere, Nature, 395, 486-490, 1998.
Wahner, A., A.R. Ravishankara, S.P.Sander, and R.R.Friedl, Absorption cross section of BrO between 312 and 385 nm at 298 and 223K, Chem. Phys. Lett., 152, 507-512, 1988.

F.2. Technical notes

ESA 2004: Algorithm Theoretical Basis Document for GOME Total Column Densities of Ozone and Nitrogen Dioxide, UPAS/GDOAS: GDP 4.0, ESA Technical Note ERSE-DTEX-EOPG-TN-04-0007, Ed. By DLR, Iss./Rev. 1/A, 15 December 2004. [http://earth.esrin.esa.it/pub/ESA_DOC/GOME/]

De Smedt, I., M. Van Roozendael, T. Jacobs: Optimization of DOAS settings for BrO fitting from SCIAMACHY nadir spectra - Comparison with GOME BrO retrievals, Technical note in support of the SCIAMACHY Algorithm Development and Data Usage (SADDU), Ed. BIRA-IASB, Brussels, Belgium, 10 February 2004.

Theys, N., M. Van Roozendael, Q. Errera, S. Chabrillat, F. Daerden, F. Hendrick, D. Loyola, and P. Valks, BrO column retrieval algorithms for GOME-2, Ozone-SAF Visiting Scientist final report, DLR-IMF, Oberpfaffenhofen, Germany, 2007.

Van Roozendael, M., F. Hendrick, N. Hao, C. Fayt, C. Hermans, A. Merlaud, N. Theys, D. Loyola, P. Valks, J.-C. Lambert, G. Pinardi, Initial validation of GOME-2 GDP 4.2 BrO total columns – ORR A3, Validation report, TN-IASB-GOME2-O3MSAF-BrO-01, 15 April 2008.